Lawrence Berkeley National Laboratory
Recent Work

Title
SEM HOT STAGE SINTERING OF U02.

Permalink
https://escholarship.org/uc/item/9f33z0j6

Author
Miller, Daniel John.

Publication Date
1976-06-01

SEM HOT STAGE SINTERING OF UO_2
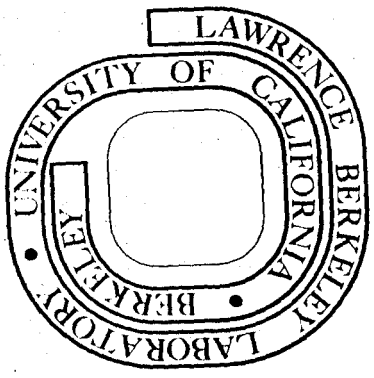
Daniel John Miller
(M. S. thesis)

June 1976

DISCLAIMER

SEM HOT STAGE SINTERING OF UO_2

Contents

SEM HOT STAGE SINTERING OF UO_2

Daniel John Miller

Materials and Molecular Research Division, Lawrence Berkeley Laboratory
and Department of Materials Science and Engineering,
University of California, Berkeley, California   94720

ABSTRACT

The sintering of hyperstoichiometric uranium dioxide powder

compacts, in the hot stage of the scanning electron micriscope, was

continuously monitored using 16 mm time lapse movies. From alumina

microspheres placed on the surface of the compacts, shrinkage measure-

ments were obtained. Converting shrinkage measurements into densifica-

tion profiles indicates that a maximum densification rate is reached at

a critical density, independent of the constant heating rates.

At temperatures above 1350°C, the movement of the reference

microspheres made shrinkage measurements impossible. It is believed

the evolution of UO_3 gas from hyperstoichiometric UO_2 is the cause of

this limitation.

INTRODUCTION

Uranium dioxide is a refractory ceramic material of vital importance to the nuclear energy industry. Most commercial, thermal, nuclear reactors generate power using rods of uranium dioxide as the fuel material. The characteristics of high melting temperature (~2865°C), resistance to irradiation damage, and general stability in the demanding reactor environment outweigh the low thermal conductivity of UO_2 to make it the preferred uranium bearing compound for the fuel matrix.

Uranium oxide is incorporated into reactors in the form of dense (>90% TD), cylindrical pellets stacked in a metallic cladding, commonly a zirconium alloy or stainless steel. As with many ceramic materials, the most economical method of producing dense UO_2 pellets is by cold pressing a fine powder of this material and sintering at elevated temperatures.

The microstructure which results from sintering is intimately related with the performance of the fuel element. Remnant porosity reduces thermal conductivity and thereby decreases the available power output. Fuel pellets containing pores may further densify while in service in a reactor. The rearrangement of fuel material results in nonuniform fuel elements and related problems in controlling the fission reaction. The grain size of the sintered UO_2 is known to influence swelling and fission gas release[1] as well as strength and fracture characteristics.[2] An understanding of the sintering processes of UO_2, from the initial, pressed density to the final developed microstructure is important, therefore, in economically fabricating fuel elements of maximum energy efficiency.

The driving force for the sintering of powder compacts is the elimination of excess surface free energy. In ceramic systems that sinter without the presence of a liquid phase, surface free energy is reduced by solid state diffusion mechanisms. The shrinkage of a particulate compact will result from volume diffusion and grain boundary diffusion. Due to the complexities of the process, however, no generally accepted sintering theory exists at this time.

Quantitative solutions for the reduction of surface area in model systems consisting of regular arrangements of spherical particles have been offered by a number of investigators.[3, 4, 5] Comparison of shrinkage equations with experimental measurements has often been used to interpret initial sintering data of powder compacts neglecting the restrictions inherent in the models. The investigations of Exner et al.[6] and Shumaker and Fulrath[7] indicate that initial solid state sintering cannot be so simply treated due to non-uniform particle packings and particle rearrangements.

The latter stages of sintering, in which a continuous pore phase shrinks and forms isolated pores, was modeled by Coble[8] with the assumption of pores of uniform size, shape and distribution. Agglomerations of fine particles, grain growth, Ostwald ripening of pores and many other processing and densification parameters affecting kinetics negate the acceptability of such models to actual ceramic powder compacts. A statistical approach to sintering has recently been suggested as an alternative to models which assume well defined microstructural geometries.[9]

Due to the variety and limitations of experimental techniques, descrepancies exist among the results of different sintering investigations.

Sintering is often studied through shrinkage measurements obtained during isothermal conditions at various elevated temperatures. The inability of studying the rapid initial shrinkage while isothermal conditions are being established is a major difficulty of this technique. The rapid heating of specimens to high temperatures will also cause stresses in the material which may have effects on the measured shrinkage. These problems can be eliminated by continuously measuring shrinkage during a constant rate of heating. Such experiments also more nearly approach industrial sintering conditions.

The intricacies of solid state sintering of ceramic powder compacts are further complicated for UO_2* by the strong tendency for formation of higher oxide phases and resulting nonstoichiometry. The diffusivities of both uranium ions and oxygen ions are greatly increased as oxygen enters the flourite lattice of stoichiometric UO_2.[10,11] Attention must be given, therefore, to the effects of composition and changes in composition which may influence the sintering kinetics of UO_2.

This report presents the initial work on the sintering of UO_2 studied by hot stage scanning electron microscopy. Shrinkage was continuously monitored at various constant heating rates to avoid the problems which accompany isothermal methods. The use of three constant heating rates provided information on the densification of UO_2 without the assumptions of model behavior.

*Throughout this report, UO_2 will refer to a hyperstoichiometric UO_2.

EXPERIMENTAL

A. APPARATUS

The modification of a commercial hot stage to give magnifications

from 50 to 5,000X at temperatures up to 1600°C and the operation of this

hot stage in the scanning electron microscope* has been reported by

Fulrath.[12]

Hot stage scanning electron microscopy has proved to be an effective

method of studying both solid state[7,13] and liquid phase sintering.[14, 15]

The increased statistical capabilities of studying the densification of

a particulate compact from constant visual inspection of its surface at

high temperatures is the main advantage of this technique when compared

with other methods. A limitation exists, however, in the necessity of

a vacuum environment for operation of the SEM.

The specimen stage carrier used in this study is shown in Fig. 1.

A 15 mil thoriated tungsten wire wound on a high purity alumina tube

(99.8%) jacketed in an outer alumina sleeve forms the heating element.

Platinum crucibles used in this study were supported within the heating

element by a molybdenum stand. A 5 mil, W5% Re-W26%Re thermocouple

was spot welded to the bottom of the stand to provide temperature

measurements. The accuracy of temperature measurement was ±15°C as

determined by optical pyrometry. The deviation of the UO_2 compact

temperature from the measured value was essentially constant, however,

during a sintering run. Molybdenum radiation shields surrounding the

heating element and placed over the top prevented excessive radiant

*JEOL JSM-U3

heat losses. Electrical connections of the specimen stage are isolated from the metal frame block by alumina plates.

MATERIAL AND SAMPLE PREPARATION

The UO_2 of this study was obtained in the form of cylindrical pellets of specified size for hot stage work (~.18 in. dia. × 1 in. height)[*]. The pellets were formed in a hardened tool steel die, lightly lubricated with a stearic acid solution, at 25,000 psi utilizing uniaxial pressing techniques. The pellets contained no binding additions, an important fact as organic binders have shown to be detrimental to the densification of UO_2.[16] As pressed densities were calculated from micrometer measurements and dry weights. Green pellets were 50% TD ± 2% (TD = 10.97 g/cc). The O/U ratio was 2.18 as determined by oxidation of the material to U_3O_8 at 750°C in air. From micrographs of fractured green pellets, the particle size was observed to range between 1000Å and 5000Å.

Alumina microspheres (10-15μm), placed on the surface of the prepressed pellets served as reference points for shrinkage measurements. By lightly tapping a glass slide, on which a small amount of alumina was placed, over a pellet within a Pt crucible, a random distribution of the fine microspheres was obtained. A metal rod was used to lightly press the microspheres onto the surface to insure their stability. The crucible and pellet were placed in the sample stage carrier and inserted into the SEM.

[*]UO_2 provided by G. E. Co., Nuclear Energy Division, Vallicitos, CA.

SHRINKAGE MEASUREMENTS

The UO_2 pellets were heated to 500°C in the SEM and held at temperature. An area suitable for shrinkage measurements was located and the instrument focused. A low magnification of approximately 100 X at which shrinkage was measured was also fixed at this time. Low magnification was used to obtain a good statistical shrinkage measurement over a large surface area. Higher magnification was used to keep the area of study centered during densification. The pellet was kept in focus during dimensional changes by raising and lowering the specimen stage within the SEM. This technique eliminated any magnification changes accompanying focal adjustments.

Constant heating rates of 2, 4 and 8°C/min were used from 500°C to temperatures of 1600°C. A 16 mm movie camera was used to record the TV scanning image at 20°C intervals during temperature rise. Continuous shrinkage was determined by projecting the time lapse films on a wall and measuring distances between specific microspheres. At least five measurements at each 20°C interval provided an average shrinkage of the specimen. Figure 2 illustrates how the dimensional changes between microspheres provide a measure of compact shrinkage.

Shrinkage values were converted into density values from:

$$\rho = \frac{\rho_g}{\left(\frac{\ell - \ell o}{\ell o}\right)^3}$$

where ρ = relative density of sample

ρ_g = relative green density (.50 used in all calculations)

ℓo = Length between two spheres before shrinkage

ℓ = Length between spheres at temperature

RESULTS AND DISCUSSION

The shrinkage and corresponding densification profiles of the UO_2 compacts as functions of heating rate and temperature are shown in Figs. 3 and 4. Shrinkage commences between 650°C and 750°C, depending upon heating rates. Shrinkage measurements above 1340°C were not possible due to movements of the Al_2O_3 microspheres. An explanation of this phenomenon will be offered later. The S-shaped curves of Figs. 3 and 4 indicate that a maximum densification rate is reached before 1340°C during all three constant rates of heating. The densification rate was calculated using measurements of the slope of the relative density versus temperature curve at 20°C intervals from:

$$\frac{d\rho}{dt} = \frac{d\rho}{dt} \times a$$

where
$$\frac{d\rho}{dt} = \text{densification rate}$$

$$\frac{d\rho}{dt} = \text{measured slope}$$

$$a = \text{constant heating rate}$$

Densification rate as a function of temperature and constant heating rate is shown in Fig. 5. The densification rate is a maximum at approximately 1000°C, 1060°C, and 1110°C for constant heating rates of 2, 4, and 8°C/min respectively. Referring back to Fig. 4, it can be seen that at these approximate temperatures the samples are of equivalent densities. A plot of densification rate vs. relative density clearly correlates these parameters. Figure 6 indicates that, the UO_2 of this study undergoes a maximum densification rate at a density of approximately 65% TD, independent of heating rate. The occurrence of this

maximum at a critical density stresses the importance of the developing microstructure on sintering kinetics.

Studies of both uranium and oxygen diffusion have been reviewed by Belle.[10] The diffusivity of oxygen is many orders of magnitude greater than the diffusivity of uranium in the oxide of stoichiometric composition and in oxides containing excess oxygen.[10,11] It is generally accepted, therefore, that the sintering of UO_2 is kinetically limited by the diffusion of the cation, although plastic flow has also been considered a mechanism of densification.[17]

Diffusion mechanisms and activation energies for the sintering of UO_2 have been proposed in a number of studies by fitting initial sintering data to model equations. The results of some of these studies are presented in Table I.

The range of activation energies in both diffusion and sintering studies have been inconsistent with changes in O/U ratio. A rationalization of the discrepancies is a difficult task. The poor agreement of those studies is an indication of the dependence of the findings upon material characteristics, experimental technique and analytical method.

An apparent activation energy for the sintering of the hyperstoichiometric UO_2 of this study was determined from:

$$\frac{d\rho}{dt} = \frac{k \exp\ (^-Q/RT)}{T}$$

where $\frac{d\rho}{dt}$ = densification rate

k = constant related to properties of the UO_2

T - Temperature °K

R = Gas constant

$\dot{Q}$ = Apparent activation energy

TABLE I. Results of UO$_2$ Sintering Studies

Material	Atmosphere	Activation Energy (kcal/mole)	Proposed Mechanism	Reference
UO$_{2+X}$	Flowing Ar	65.8±6.2	Uranium Volume Diffusion	Amato et al. (18)
UO$_2$ & UO$_{2+X}$	Flowing H$_2$ and CO$_2$/CO	107±11	Uranium Volume Diffusion	Lay and Carter (19)
UO$_{2.08}$	Flowing Co$_2$/CO	55	Uranium Volume Diffusion	Lay (20)
UO$_2$	Flowing H$_2$	86±8	Uranium Grain Boundary Diffusion	Woolfrey (21)

Inherent in this equation is the independence of densification rate

from heating rate. In other words, the rate of densification is depend-

ent upon temperature but not density. In Fig. 5, this is seen to be

true for compacts densifying at constant heating rates of 2°C/min. and

4°C/min. Before the critical density is reached, the densification

rates for both heating rates follow the same curve. The densification

rates for the fastest heating rate, however, are always higher than

those for the slower heating rates.

An Arrehnius plot of densification rate versus reciprocal temperature

was made to obtain the apparent activation energy of the sintering pro-

cess. This plot, shown in Fig. 7, shows a constant exponential de-

pendence of densification rate upon temperature until the critical den-

sity is approached. A value of 23 kcal/mole for the apparent activation

energy was calculated for all three heating rates. Since the temperature

dependence of the densification rate is independent of heating rate, it

can be concluded that the sintering of the UO_2 used in this study occurs

by the same diffusional processes under the three constant heating rates

employed.

The maxima of the curves of Fig. 7 correspond to the maximum

densification rates which occur during the three constant rates of

heating at 65% relative density. The changes in slope of these curves

indicates that after the UO_2 compacts have reached this critical density,

densification rate is dependent upon density. A change in the rate

controlling mechanism for the sintering process, i.e. a change in the

activation energy for sintering might also contribute to the changes

in the slopes of the curves of Fig. 7. A change in sintering mechanism

alone, however, could not explain the reversal in the sign of these slopes.

The 23 kcal/mole value is much lower than values previously reported for the activation energy for uranium diffusion in hyperstoichiometric UO_2 (see Table I). This value is in good agreement with the activation energy for oxygen diffusion in hyperstoichiometric UO_2.[23,24] It should be noted, however, that the apparent activation energy of the sintering process in which fine particles may densify by various diffusional mechanisms in concert is not unquestionably comparable with activation energies determined on single crystal or dense polycrystalline samples used in diffusion studies.

Activation energies calculated for the sintering process are dependent upon the sintering rate equation as derived from empirical data or as assumed from model experiments. Woalfrey and Bannister modified the general, model equation for isothermal initial stage sintering for application to constant heating rate experiments.[22] Using nonisothermal techniques, these investigators calculated an activation energy of 85±8 kcal/mole for the initial stage sintering of UO_2. From the data they present, it is evident this activation energy was obtained by multiplying an effective value of approximately 24 kcal/mole by a critical exponential value correlating shrinkage rate with shrinkage in the sintering rate equation. The close agreement of the activation energy for this study with the effective activation energy determined from Woolfrey and Bannister's results supports the validity of the shrinkage measurements obtained using the hot stage technique. The deviation of the highest heating rate data from the empirical formula

used to calculate the apparent activation energy suggests further study to more precisely determine the dependence of densification rate upon changes in density. The 23 kcal/mole value of this study is presented, therefore, as an effective activation energy for the sintering of UO_2.

Shrinkage measurements of hyperstoichiometric UO_2 at temperatures above 1350°C were not possible using hot stage scanning electron microscopy due to movement of the reference alumina microspheres. This effect is believed to be a result of the chemical instability of UO_2 at these temperatures and the resulting evolution of a gaseous uranium bearing species.

During sintering of the UO_2 pellets, at temperatures of approximately 1400°C, a decrease in resolution of the SEM picture was noted; possibly due to the evolution of a gas phase. In analyzing the sintering films, it was also noticed that at these same temperatures the Al_2O_3 microspheres moved from their initial positions in a haphazard manner. After constant heating to temperatures of 1500°C, a gray deposit was observed on the molybdenum radiation shields. X-ray diffraction of the shields revealed peaks for uranium oxides. The low intensity of these peaks and the overlap of identifiable peaks for uranium oxides, however, prevented the exact determination of the phase present.

The volatility of hyperstoichiometric UO_2 at high temperatures in the SEM is supported by the investigation of Chapman and Meadows.[25] Using thermogravimetry they studied the volatility of pressed, unsintered pellets of UO_2 with O/U ratios ranging from 2.10 to 2.18 at system pressures of 10^{-5} to 10^{-6} torr. The hot stage is operated in the SEM in a vacuum of approximately 3×10^{-5} torr. At temperatures as low as

1125°C, Chapman and Meadows observed a measurable loss of uranium. As temperature was increased to 1500°C, the rate of weight loss increased until the samples neared stoichiometric compositions.

The incongruent vaporization of hyperstoichiometric UO_2 will yield oxygen and a gaseous trioxide.[26] The evolution of UO_3 gas from hyperstoichiometric UO_2 was an observation in the vacuum sintering study of Williams, et al.[17]

The question must be asked if the densification behavior reported in this study was possibly influenced by compositional changes of the UO_2.

The influence of hyperstoichiometry on the diffusivities of oxygen and uranium in UO_2 has been reported.[10,11] These studies indicate that a small increase in interstitial oxygen content over the stoichiometric composition profoundly enhances both uranium and oxygen diffusion. The sensitivity of the ionic diffusivities to excess oxygen decreases as the degree of hyperstoichiometry increases. These results support the findings of sintering studies in which slight departure from stoichiometry greatly increases the sinterability of a material. In the investigation of Williams, et al., no further beneficial effect was observed with increases of oxygen content beyond $UO_{2.03}$.

Chapman and Meadows suggest from their results that compositional changes of hyperstoichiometric UO_2 below 1125°C, in a system similar to the one used in this study, result from the slow loss of oxygen. They state that at 1000°C virtually no reaction takes place. The effective activation energy for sintering reported in this study was calculated from shrinkage measurements in the temperature range 780°C to

1060°C. Due to the high degree of nonstoichiometry of the UO_2 (O/U=2.18) and the short period of time at temperatures where compositional changes are reported as being kinetically slow, it is believed the activation energy of this study was not affected by compositional changes.

The occurrence of the maximum densification rate at a critical density might also be suspected of being a spurious result due to compositional changes of the UO_2. A similar dependence of densification rate upon density has been found, however, for Linde-A alumina powder compacts.[13] This fact lends support to the findings of this study and to the criticality of microstructural effects of sintering kinetics in particle compaces.

CONCLUSIONS

The hyperstoichiometric UO_2 of this study was found to undergo a maximum densification rate at a density of 65% T.D. independent of three constant heating rates employed. The equivalent exponential dependence of densification rate upon temperature up to the critical density suggest the mechanisms of sintering are unchanged by constant heating rates.

From observations of this study and a review of results of studies on similar systems, it is concluded that the study of sintering of UO_2 by hot stage scanning electron microscopy is limited by compositional changes at high temperatures in the vacuum of the SEM. To confirm the results of this study, shrinkage must be monitored with careful control of the O/U ratio of the material.

ACKNOWLEDGMENT

-17-

REFERENCES

1. J. A. Turnbull, "The Effect of Grain Size on the Swelling and Gas Release Properties of UO_2 During Irradiation", J. Nucl. Mat. 50, 62-68 (1974).

2. A. G. Evans and R. W. Davidge, "The Strength and Fracture of Stoichiometric Polycrystalline UO_2", J. Nucl. Mat. 33, 249-260 (1969).

3. D. L. Johnson, "New Method for Obtaining Volume, Grain Boundary and Surface Diffusion Coefficients from Sintering Data", J. App. Phys. 40 [1], 192-200 (1969).

4. R. L. Coble, "Initial Sintering of Alumina and Hematite", J. Am. Ceram. Soc. 41 [2], 55 (1958).

5. D. L. Johnson and I. B. Cutler, "Diffusion Sintering I, Initial Stage Sintering Methods and Their Application to Shrinkage of Powder Compacts", J. Am. Ceram. Soc. 46 [11], 541-545 (1963).

6. H. E. Exner, G. Petzow and P. Wellner, "Problems in the Extension of Sintering Theories to Real Systems", Materials Science Research volume 6, "Sintering and Related Phenomena, 351-362, Plenum Press, NY (1973).

7. C. B. Shumaker and R. M. Fulrath, "Initial Stages of Sintering of Copper and Nickel", ibid. 191-199.

8. R. L. Coble, "Sintering Crystalline Solids. I. Intermediate and Final State Diffusion Models", J. App. Phys. 32 [5], 787-792 (1961).

9. G. C. Kucynski, "Statistical Approach to the Theory of Sintering", Materials Science Research, volume 10 "Sintering and Catalysis", 325-337, Plenum Press (1975).

10. J. Belle, "Oxygen and Uranium Diffusion in Uranium Dioxide (A Review)", J. Nucl. Mat. $\underline{30}$ [4], 3-15 (1969).

11. J. F. Marin and P. Contamin, "Uranium and Oxygen Self-Diffusion in UO_2", $\underline{ibid.}$ 16-25.

12. R. M. Fulrath, "Scanning Electron Microscopy to 1600°C", Proceedings of the Fifth Annual Scanning Electron Microscope Symposium (ITT Research Institute, 1972), p. 17.

13. D. N. K. Wang (personal communication).

14. L. Froshauer and R. M. Fulrath, "Direct Observation of Liquid-Phase Sintering in the System Iron-Copper", J. Mat. Sci. $\underline{10}$, 2146-2155 (1975).

15. L. Froshauer and R. M. Fulrath, "Direct Observation of Liquid-Phase Sintering in the System Tungsten Carbide-Cobalt", J. Mat. Sci. $\underline{11}$, 142-149 (1976).

16. J. Williams, "Sintering of Uranium Oxides", J. Nucl. Mat. $\underline{2}$, 92-93 (1960).

17. J. Williams, E. Barnes, R. Scott and A. Hall, "Sintering of Uranium Oxides of Composition UO_2 to U_3O_8 in Various Atmospheres", J. Nucl. Mat. $\underline{1}$, 28-38 (1959).

18. I. Amato, R. L. Colombo, and A. M. Protti, "On the Activation Energy of Sintering Non-Stoichiometric Uranium Oxide", J. Nucl. Mat. $\underline{11}$ [2], 229-235 (1964).

19. K. W. Lay and R. E. Carter, "Role of the O/U Ratio on the Sintering of UO_2", J. Nucl. Mat. $\underline{30}$, 74-87 (1969).

20. K. W. Lay, "Initial Sintering Kinetics of Hyperstoichiometric Uranium Dioxide", J. Amer. Cer. Soc. 54 [1], 18-21 (1971).

21. J. L. Woolfrey, "Effect of Green Density on the Initial-Stage Sintering Kinetics of UO_2", J. Amer. Ceram. Soc. 55 [8], 383-389 (1972).

22. J. L. Woolfrey and M. J. Bannister, "Nonisothermal Techniques for Studying Initial Stage Sintering", ibid. p. 390-394.

23. P. Contamin, J. J. Bacmann and J. F. Marin, "Autodiffision de l'Oxygene dans le Dioxide d'Uranium Surstoechiometrique", J. Nucl. Mat. 42, 54-64 (1972).

24. K. W. Lay, "Oxygen Chemical Diffusion Coefficient of Uranium Dioxide", J. Amer. Ceram. Soc. 53, [7] 269-373 (1970).

25. A. T. Chapman and R. E. Meadows, "Volatility of $UO_{2 \pm x}$ and Phase Relations in the System Uranium-Oxygen", J. Amer. Cer. Soc. 47 [12] 614-621 (1964).

26. "Thermodynamic and Transport Properties of Uranium Dioxide and Related Phases", IAEA Technical Report Series No. 39, Vienna (1965).

FIGURE CAPTIONS

Fig. 1.   Hot Stage Specimen Carrier.

Fig. 2a.   Alumina Microspheres on UO_2 Pellet at 650°C.

Fig. 2b.   Alumina Microspheres on UO_2 Pellet at 1100°C.

Fig. 3.   Shrinkage of UO_2 Powder Compacts at Various Constant

Heating Rates.

Fig. 4.   Densification Profiles of UO_2 Powder Compacts at Various

Constant Heating Rates.

Fig. 5.   Densification Rate of UO_2 Powder Compacts as Function of

Temperature and Constant Heating Rates.

Fig. 6.   Densification Rate vs. Density for UO_2 Powder Compacts

Sintered During Various Constant Heating Rates.

Fig. 7.   Plot of $\ln(T)(\frac{d\rho}{dt})$ vs. 1/T for Sintering of UO_2 Powder Compacts.
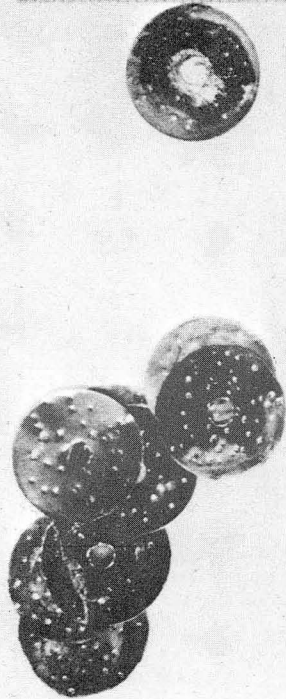
TOP RADIATION SHIELDS
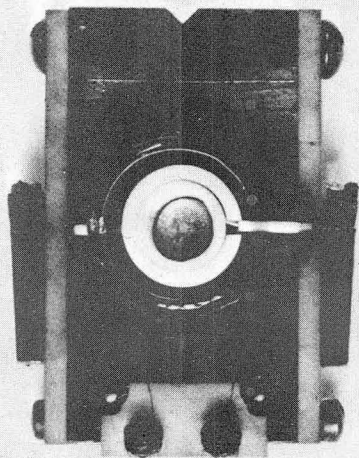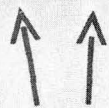
THERMOCOUPLE CONNECTIONS

HEATER CONTACT

TOP SHIELD

MO - CRUCIBLE

Fig. 1

(a)
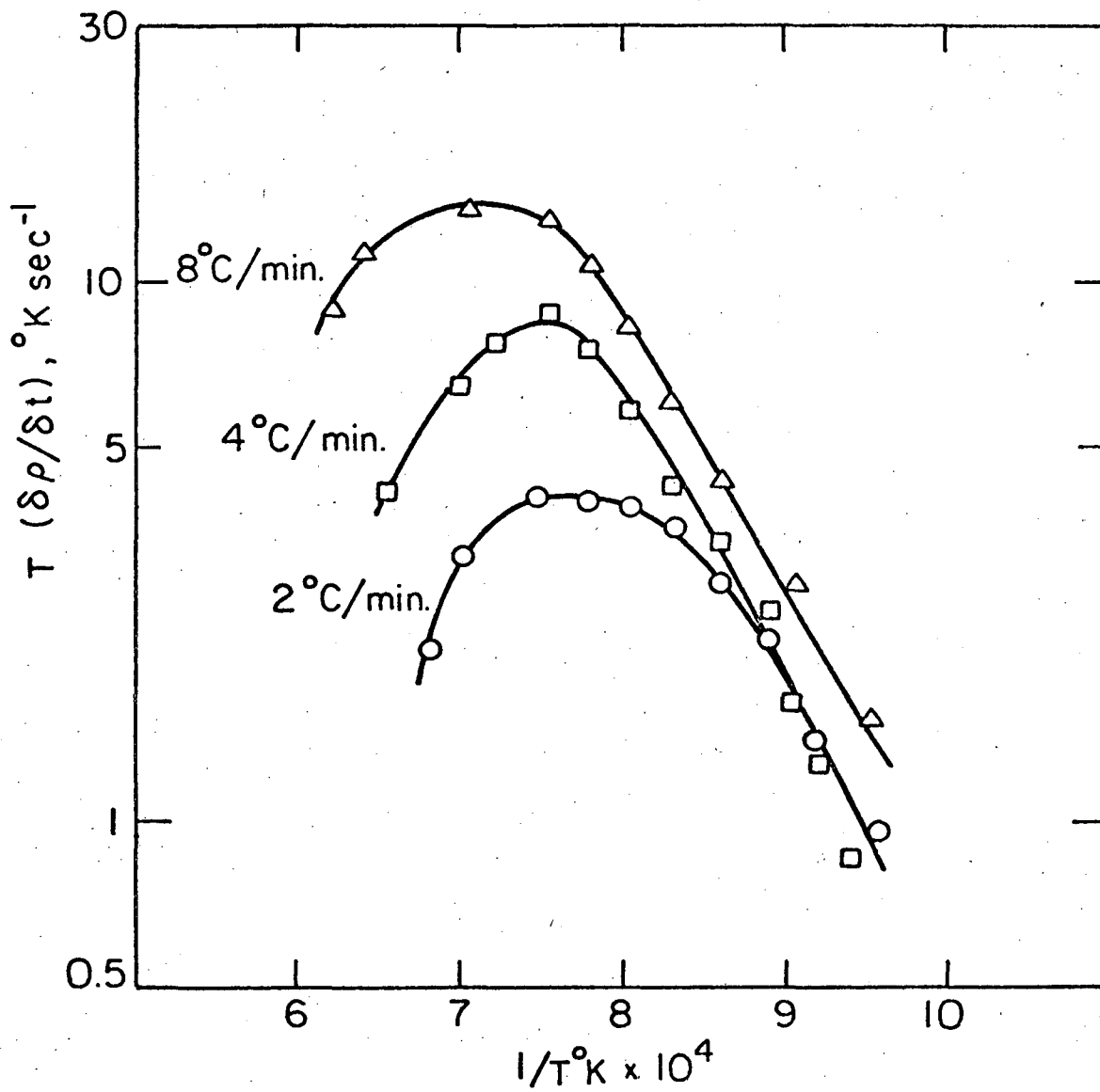
50 μ

(b)

50 μ
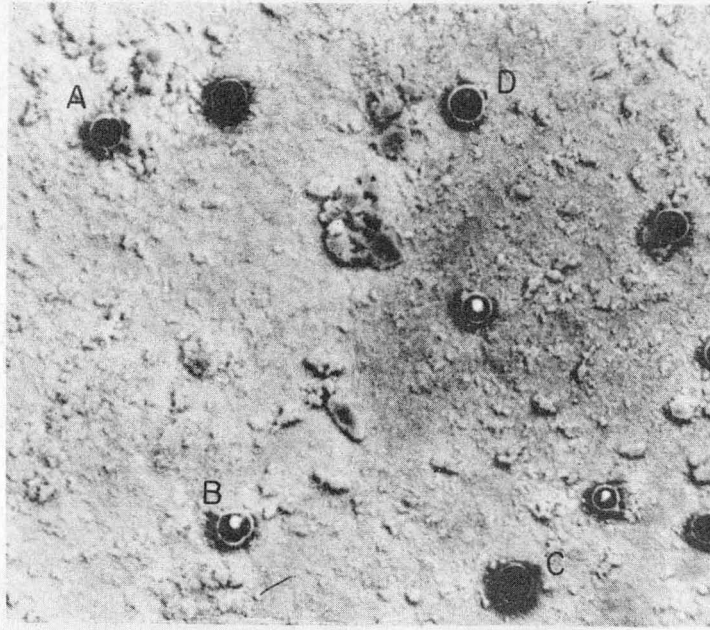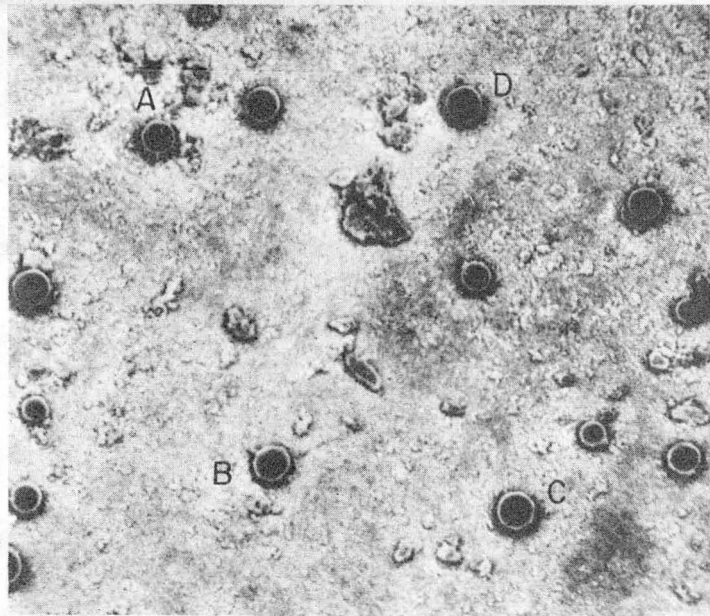
XBB766-4822

Fig. 2
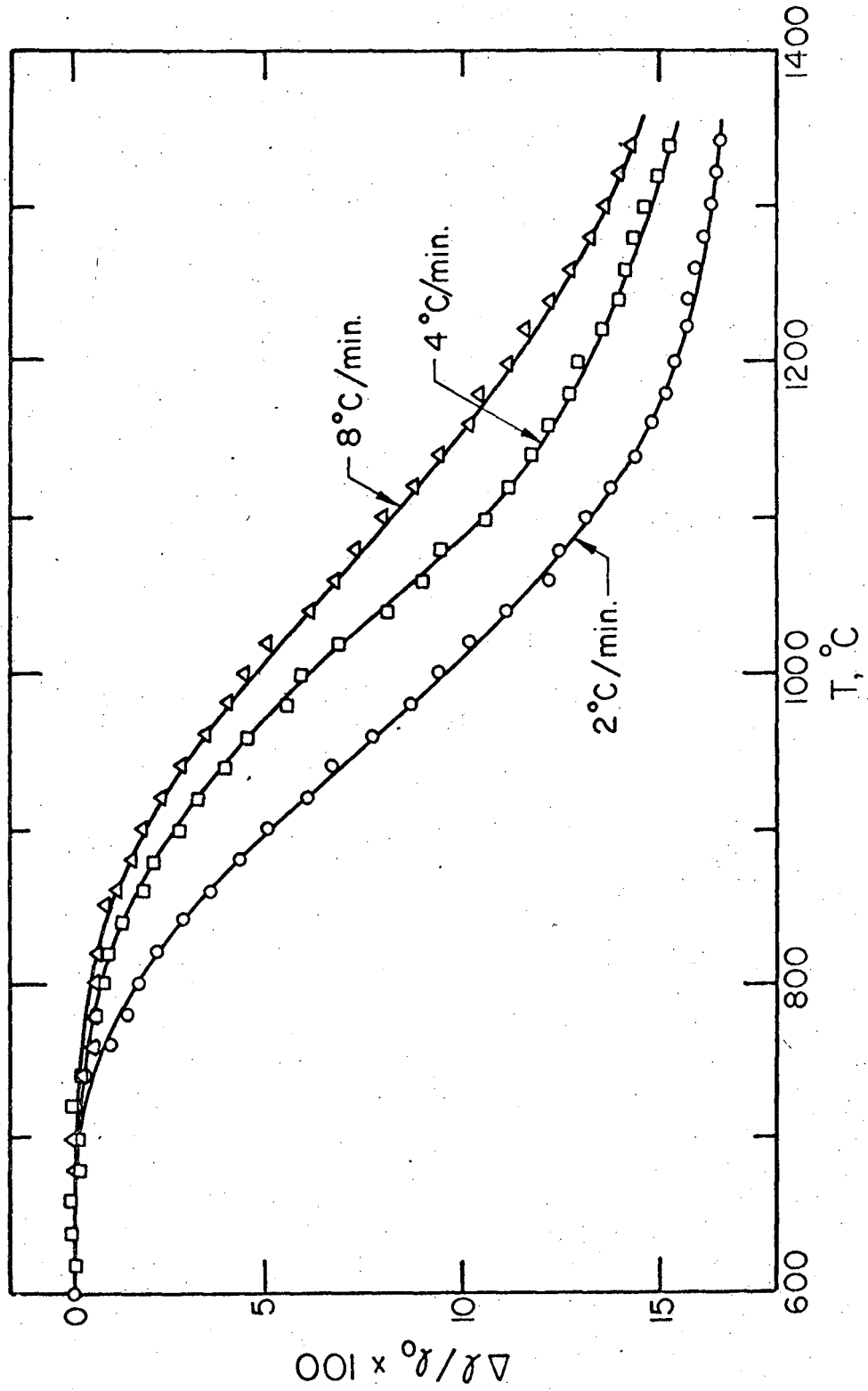
XBL759-7378

Fig. 3
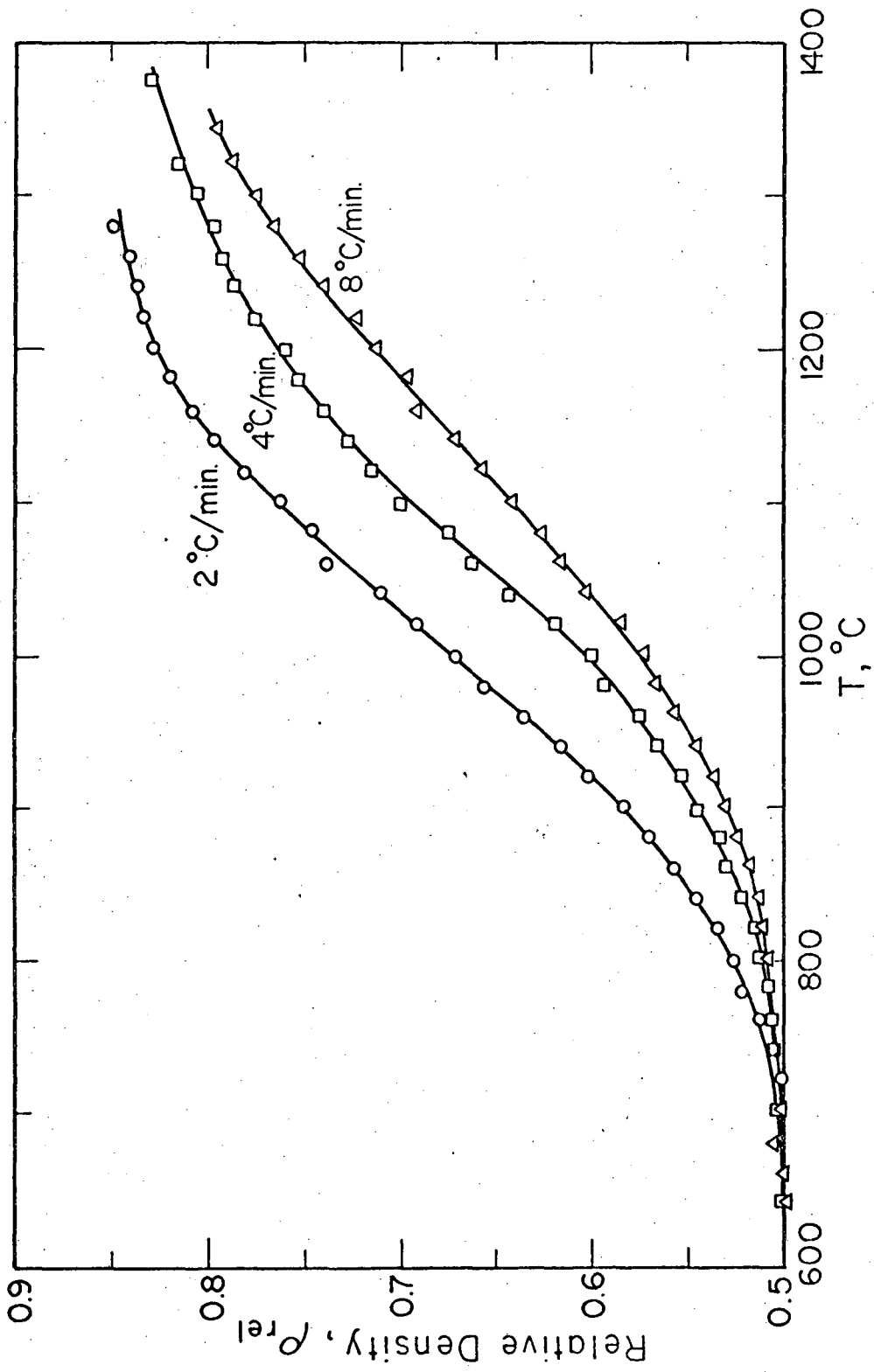
XBL 759-7379

Fig. 4
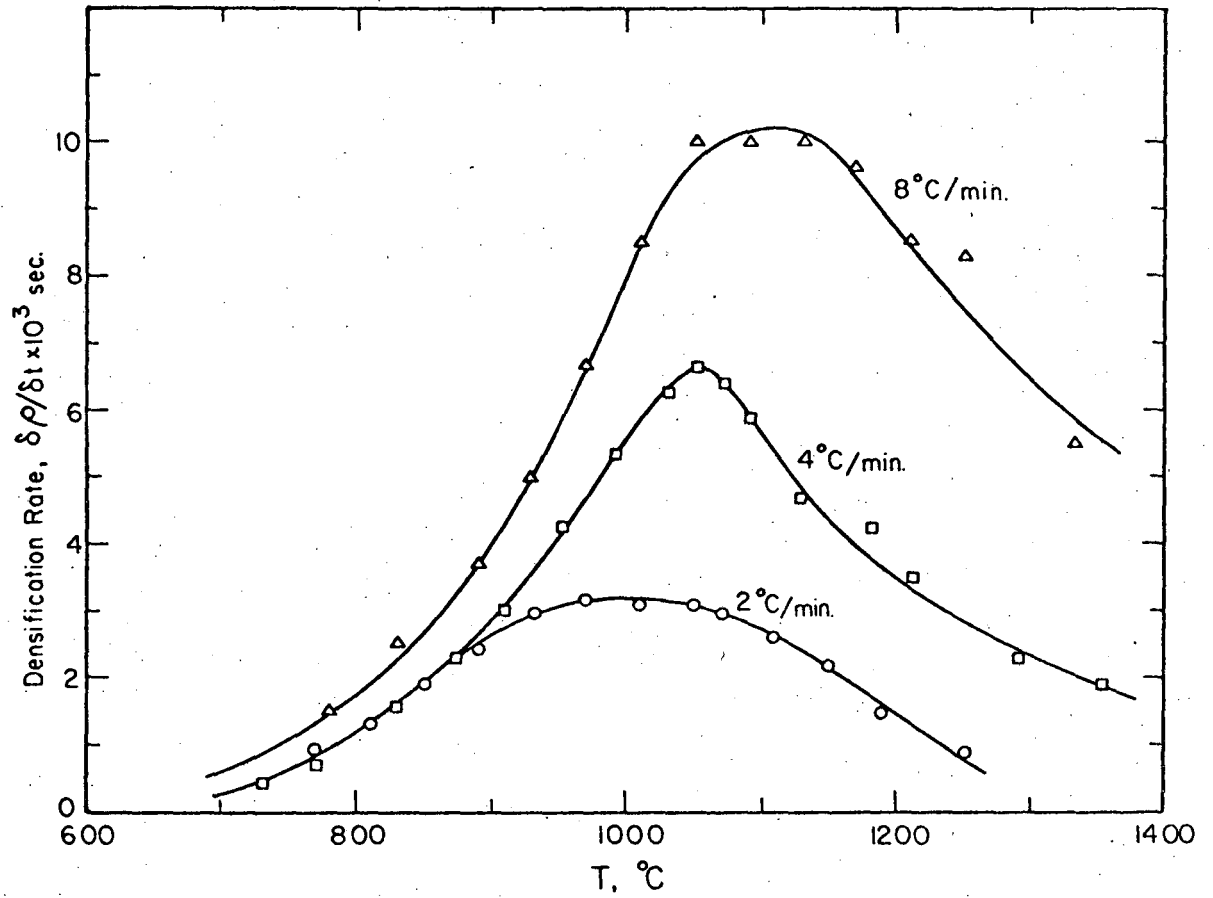
XBL759-7377

Fig. 5

XBL 759-7380

Fig. 6

XBL759-7381

Fig. 7